MIJST
MIST International Journal of Science and Technology

Physical, Mechanical, and Durability Properties of Concrete with Class F Fly Ash

Md Jahidul Islam[1*], Tasnia Ahmed[2], Md Riadus Salehin[3], Mohammad Sadman Sakib[4], Md Shakil Shariar[5], and Monowar Hossain[6]

Department of Civil Engineering, Military Institute of Science and Technology, Dhaka, Bangladesh

emails: *[*1]mjislam@ce.mist.ac.bd; [2]tasnia@ce.mist.ac.bd; [3]salehin_75@yahoo.com; [4]ssakibbd@yahoo.com; [5]shakil.otj@gmail.com; and [6]monowar5478@gmail.com*

ARTICLE INFO

Article History:

Received: 19th May 2023
Revised: 17th August 2023
Accepted: 21st August 2023
Published: 28th December 2023

Keywords:

Class F fly ash
Microstructure
Splitting tensile strength
Modulus of elasticity
Durability properties

ABSTRACT

Concrete is one of the most used manufactured materials in the world. Fly ash (FA) is a byproduct produced from pulverized coal combustion in power generation. A total of 0.08 million tons of class F fly ash is produced from a coal-based power plant yearly in Barapukuria, Bangladesh, whose disposal is of a great issue. Therefore, this study aims to explore the possibility of using class F FA in concrete construction as a supplementary cementitious material. In this study, two different water-to-cement ratios (0.4 and 0.5), each with five cement replacement levels numerically, 0%, 10%, 20%, 30%, and 40% with FA are used. Various tests are performed on cylinder and beam specimens to assess physical, mechanical, and durability properties, such as workability, density, compressive strength (CS), splitting tensile strength (STS), flexural strength (FS), chloride ion penetrability (CIP), and shrinkage. Analyzing the results, it is reported that workability increases and density decreases with the increasing FA replacement. Mechanical properties mostly decrease with increasing FA content. However, the strength gained with age is higher for concrete with FA compared to the control concrete. The CIP reduces with FA replacement, especially at 56 days of age. Shrinkage value reduces 82% at 40% replacement FA replacement and w/c ratio 0.4. However, at 10% FA replacement and concrete age of 56 days, mechanical strength loss is infinitesimal or even better compared to the control concrete. Thus, a low replacement percentage of FA with a high curing period is a suitable concrete cement alternative.

1. INTRODUCTION

The modern world is largely dependent on concrete for urbanization and development processes. Cement is a crucial binding material that requires large quantities to produce concrete, and its manufacture demands the use of substantial resources and energy. It also produces many types of harmful emissions, causing environmental effects. Cement production is one of the biggest contributors to carbon dioxide (CO2) production (Feiz *et al.*, 2015), accounting for about 5-7% of manmade CO2 emissions (Barcelo *et al.*, 2014). In 2021, about 35 billion tons of concrete and 4.4 billion tons of cement were used. The percentage of CO2 production by the cement industries can be lowered by up to 90% by reducing the cement requirement in concrete (Andrew, 2018).

Coal is responsible for around 40% of electricity generation worldwide. It is also the key source of carbon dioxide production (Breeze, 2015). Fly ash (FA), the key element of coal ash, is leading to a disposal problem and therefore, is deposited in landfills (Soni *et al.*, 2020; Zierold & Odoh, 2020). Bangladesh's Barapukuria 250 MW coal-based power plant produces about 80 thousand tons of FA annually, which is disposed into empty land as waste material (Howladar & Islam, 2016). If FA can replace a certain portion of cement, it will ensure making environmentally friendly concrete, a major concern nowadays.

Among many approaches to creating environmentally responsive concrete is to partly replace a certain portion of ordinary Portland cement (OPC) with FA in concrete, available in large amounts as a byproduct of coal combustion in power plants. If it is not appropriately disposed of, it will bring about water and soil pollution and pose environmental hazards (Yao *et al.*, 2015). The application of FA can lower the impact on the environment, lessen the cost and energy production of concrete (ACI 211.1-91, 1994; Jamora *et al.*, 2020), and is being widely adopted as a partial standby for cement (Ahmaruzzaman, 2010) because of being an artificial pozzolan (ACI 116R, 2000). FA, in conjunction with Portland or blended cement, can reduce early heat of hydration, improve late-age strength development, and decrease permeability (ACI 211.1-91, 1994). FA consumes a large amount of calcium hydroxide (CH) from the cement hydration development and forms denser calcium silicate hydrate (C-S-H) at a later age (Jiang *et al.*, 2020). Improving the fineness of FA results in a raised consumption level for CH (Moghaddam *et al.*, 2019). Partial replacement of OPC with FA will ensure the making of sustainable green concrete with good compressive strength (CS) and fracture toughness (Ahmaruzzaman, 2010; Golewski, 2018).

When used as a cementitious component in concrete, FA has some attributes for raw ingredients and direct concrete admixture application for its pozzolanic properties (ACI 225R, 2016; Ahmaruzzaman, 2010; Jamora *et al.*, 2020). There may be an increased tendency for air loss during mixing, transit, and placement if FA is used in a blended cement than with cement with no FA content (ACI 225R, 2016). Finer FA reduces the heat of hydration and water requirement and increases the drying shrinkages compared to coarser FA (Moghaddam *et al.*, 2019; Vimonsatit *et al.*, 2015). The hydration products generated by the reaction of FA with CH fill in the voids, which lowers the pore volume and the average diameter of pores at a longer curing age (Sun *et al.*, 2012; Wang *et al.*, 2004) and allows the movement of moisture through the concrete (S. L. Sarkar & Banerjee, 1995) resulting in dense, durable and highly workable concrete (Ahmaruzzaman, 2010; Hardjito *et al.*, 2004; Khongpermgoson *et al.*, 2020; Koodalloor Parasuraman *et al.*, 2011). Up to 20% FA replacement is found to refine the pores and improve durability; however, 30% FA has the opposite effect on durability (Wei *et al.*, 2021).

Concrete samples containing FA show finer cracks subjected to cracking loads than samples without FA; hence, adding FA improves damage prevention (Chindasiriphan *et al.*, 2020; Khan *et al.*, 2021). It also makes denser concrete and enhances its characteristic strength (Khan *et al.*, 2021). The CS after 28 days of curing is lesser and decreases abruptly with the rise of FA content; however, it increases progressively at a later age due to the pozzolanic reaction (Saha, 2018; Wei *et al.*, 2021). A substantial increase in CS was observed at later ages, with 40% FA replacement. Furthermore, the sulfate resistance was improved up to 30% FA replacement of cement but decreased beyond the 30% level (Koodalloor Parasuraman *et al.*, 2011; Wei *et al.*, 2021). In addition, 60% replacement of OPC with FA showed a two-fold improved CS after 56 days than 28 days (Laxman Kudva *et al.*, 2022). Concrete containing up to 15% class F FA shows better CS and splitting tensile strength (STS) than concrete with only OPC as the binder (Islam *et al.*, 2023), as well as comparable long-term strength gain as high-performance concrete made with cement and class C FA (Khongpermgoson *et al.*, 2020).

It is approximated that each 10% increment of FA should let a water reduction of 3% at minimum (Thomas, 2007). The optimum value of FA is about 30%-40% of cement for normal concrete (Golewski, 2018; Islam *et al.*, 2022; Oner *et al.*, 2005) and 10% of cement for high strength concrete (Fantu *et al.*, 2021). However, the amount may vary from less than 5% to more than 40% depending on the properties of the FA and cement and the desired properties of the concrete (ACI 225R, 2016). FA mortars with low water-to-binder ratio have low drying shrinkage (Chindaprasirt *et al.*, 2004). Concrete with 10% FA as part of sand or cement exhibits the lowest drying shrinkage (Khan *et al.*, 2021; Liu *et al.*, 2022). High performance, low permeability concrete can be designed by incorporating up to 40% class F FA in the overall binder (Nath & Sarker, 2011).

The pozzolanic reaction in FA can improve concrete's self-healing capability, which develops from the newly generated C-S-H products (Chindasiriphan *et al.*, 2020). Up to the age of 3 years, a 30% FA blended cement paste develops circular voids surrounded by hydration products due to the pozzolanic reaction of hollow FA particles and is more porous than the Portland cement paste (Yu *et al.*, 2017). It can also produce lightweight concrete by acting as a lightweight aggregate (ACI 116R, 2000). About 60% of the FA mass could be separated as coarse fractions, and the remaining 40% of fine FA could be adopted as ultrafine cement after separating the carbon (Lanzerstorfer, 2018). Up to 2.85% reduction in unit weight is detected when 30% cement was substituted with FA (Fantu *et al.*, 2021).

The flexural performance of concrete beams was performed while using a high volume of FA in several kinds of research. Joanna *et al.* (Joanna *et al.*, 2020) found that the moment capacity of 50% cement-replaced FA beams is slightly more than that of the control specimens after 56 days. The strain, deflection, crack load, yield load, and ultimate load are also found to be almost similar to the content in FA (Amiri *et al.*, 2016; Chinh, 2021; Fuzail Hashmi *et al.*, 2020; Yoo *et al.*, 2015). The flexural strength of reinforced concrete beams reduces slightly after 90 days for 40% FA replacement (Chinh, 2021). The crack patterns formed in reinforced concrete beams are comparable in both with and without FA, though concrete having high volume FA shows wider cracks (Fuzail Hashmi *et al.*, 2020). Compared to ordinary concrete, the specimens containing the high volume FA layer exhibit excellent crack control (Shang *et al.*, 2021).

The above-mentioned review revealed that there is potential for using FA in concrete. However, doing an in-depth study of concrete with class F FA is essential. Therefore, this study is based on producing environment-friendly concrete by partially replacing OPC with class F FA produced from the coal-based power plant in Barapukuria, Bangladesh. Workability, density, CS, splitting tensile strength, flexural strength, and durability of concrete have been assessed where cement is replaced with 0%, 10%, 20%, 30%, and 40% FA for two w/c ratios of 0.4 and 0.5. This practice could go a long way in alleviating some of the problems or factors that affect our environment and promoting carbon-free development.

2. MATERIALS

A. Aggregates

The coarse aggregate used in this study is from Bholaganj, with a maximum size of 25 mm and a fineness modulus (FM) of 7.23. Local River sand is used as fine aggregate with a well-graded type and size between 2.36 mm to 0.075 mm with an FM of 2.71. The basic properties of the aggregates are outlined in Table 1 which are evaluated according to ASTM regulations. Figure 1 exhibits the aggregates' gradation compared to the upper and lower limits specified in the ASTM C33 (2018). Compared to fine aggregate, coarse aggregate has a higher unit weight and specific gravity.

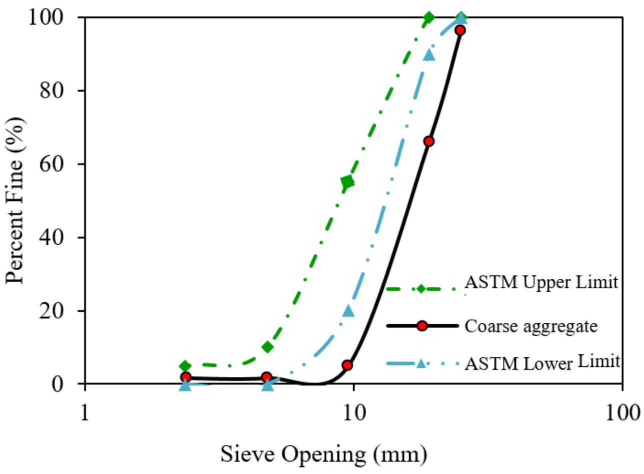

(a)

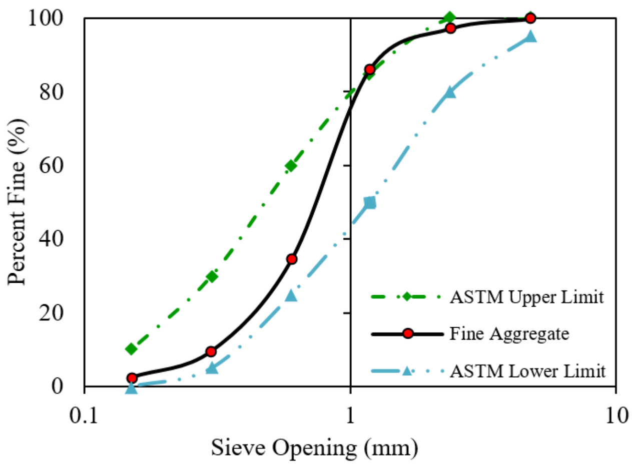

(b)

Figure 1: Particle size distribution (a) coarse aggregate (b) fine aggregate

Table 1
Basic physical characteristics of the aggregates

Component Name	Standard	Coarse Aggregate	Fine Aggregate
Maximum size (mm)	ASTM C136 (2014)	25	2.36
Fineness modulus	ASTM C136 (2014)	7.23	2.71
Specific gravity (SSD)	ASTM C127 (2015)	2.67	2.54
Absorption capacity (%)	ASTM C128 (2015)	0.33	0.60
Unit weight (kg/m^3)	ASTM C29 (2021)	1582 (compact)	1456 (compact)

B. Cement

The binding material used in the current study is ordinary Portland cement (OPC) that contains 95-100 % clinkers and 0-5% gypsum. The physical and mechanical characteristics of the cement are tested following the ASTM standards before sample preparation which is outlined in Table 2. The cement conveys a regular specific gravity and normal consistency. Compressive strength is 29.7 MPa after 28 days of curing, which is greater than 28.0 MPa, the expected value according to ASTM C150 (2021).

Table 2
Physical and mechanical characteristics of cement

Physical Properties	Standard	Result
Specific Gravity	ASTM C188 (2017)	3.15
Normal Consistency (%)	ASTM C187 (2016)	28
Compressive Strength (MPa)	ASTM C109 (2020)	29.7
Initial Setting Time (minutes)	ASTM C191 (2021)	235
Final Setting Time (minutes)		305

C. Fly Ash (FA)

Fly ash is a byproduct of coal combustion made up of particulate matter generated from coal-fired furnaces and flue gases. It can be an effective substitute for cement. It improves resistance to sulfate attack, saves cost, minimizes the hydration temperature, and lengthens the setting time. Moreover, it improves the workability of fresh concrete and produces a stronger material with less permeability (Islam *et al.*, 2023). In this study, F-class FA is used, which has a diameter of the particles ranging from 490 nm to 5.7 µm. This type of FA contains low calcium (1.56%) and has a specific gravity of 2.30, as per ASTM C188 (2017). The scanning electron microscopy (SEM) image of the FA is shown in Figure 2. Table 3 depicts the chemical analysis of FA.

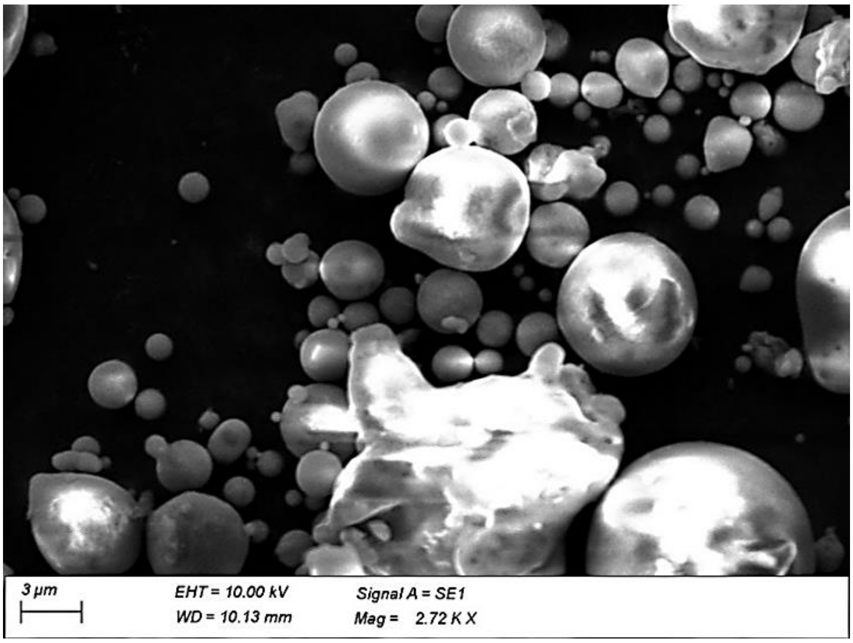

Figure 2: SEM image of FA

Table 3
Chemical analysis of FA

Components	SiO_2	Al_2O_3	Fe_2O_3	TiO_2	K_2O	CaO	P_2O_5	SO_3	Na_2O
ASTM C618 (2019) requirement (%)	Sum 50.0 (min)			-	0.8	18 (max)	-	5.0 (max)	0.7
Result (%)	54.6	28.39	5.28	5.08	1.60	1.56	1.45	0.84	0.43

3. MIX DESIGN

Using ACI 211.1-91 (1994), the mix design for concrete is prepared by replacing a different percentage of cement with FA as supplementary cementing material, varying from 10% to 40% at an interval of 10%. Samples with no FA are also prepared to compare the parameters with the typical concrete characteristics. Two distinct water-to-cement (w/c) ratios are employed, 0.4 and 0.5, eventuating in a total of 10 combinations. For studying the fresh concrete characteristics, a slump test was undertaken for every combination. Table 4 shows the quantity of various materials obtained for 1 m^3 concrete mix.

4. SAMPLE PREPARATION AND TEST PROCEDURE

Following the mix proportion mentioned in Table 4, ten combinations of the concrete mix were prepared. Saturated surface dry condition (SSD) was maintained for the aggregates. A drum-type concrete mixer machine was adopted. Initially, coarse and fine aggregates were mixed in the mixer machine for 2 – 3 minutes. Half of the water was added, followed by cement and/or FA insertion. The remaining water was poured and mixed for 2 -3 minutes. Cement and FA were mixed separately beforehand. 100 mm in diameter and 200 mm in height cylinders were made for performing compressive strength (CS), splitting tensile strength (STS), and chloride ion penetration (CIP) tests. For shrinkage and flexural strength tests, 100 mm x 100 mm x 500 mm beams have been prepared. Cylinders and beams were made in two layers, and each layer was compacted with the help of an external vibrator for about 10 seconds. Slump tests of the fresh concrete at 0 and 15 minutes were measured using a slump cone setup.

A total of 180 cylinders and 20 beams have been prepared for the whole experimental program. The CS and STS tests were performed in a 2000 kN capacity compression testing machine, as shown in Figure 3(a). A neoprene pad with a steel cap on the top and bottom face of the cylinder was used for the CS test. The CIP test was performed using a 4-point Wenner probe, known as a Resipod surface resistivity meter (Figure 3(b)). It is a non-destructive test. Hence, surface resistivity was measured for all the concrete cylinders before their respective CS and STS tests. ASTM C78 (2022) is followed to perform the flexural strength test of beam samples by third point loading. The distance between the supports at the two ends is 300 mm, keeping a clearance of 100 mm at both ends. The loading points are at equal intervals of 100 mm in between the two supports. Figure 3(c) illustrates the test setup for the flexural strength test.

5. RESULTS AND DISCUSSION

A. *Workability*

Figure 4 visualizes the result of the fresh mixture's slump test, and Figure 5 shows the comparison of slump values for different w/c ratios and FA contents. It shows that the slump value and workability improve as the FA replacement percentage increases. The control mixes with no FA have a slump value of 195 mm and 165 mm at 0 minutes and 15 minutes after casting, respectively. It increased up to 15% and 9% for 40% FA at 0 and 15 minutes. For a w/c ratio of 0.5, the workability increases by 9% and 12% for fresh and 15 minutes aged concrete. FA improves the workability because the spherical shape of the particles reduces internal friction at the interface of aggregate–paste and produces a ball-bearing effect at the contact point (Babor *et al.*, 2009; Jiménez-Quero *et al.*, 2013).

Table 4
Mix proportion for 1m^3 concrete

Designation	FA replacement (%)	w/c ratio	Water (kg)	Cement (kg)	Fly ash (kg)	Coarse aggregate (kg)	Fine aggregate (kg)
F0W4	0	0.4	193	483.0	0	957.9	711.0
F1W4	10	0.4	193	434.7	35.3	957.9	711.0
F2W4	20	0.4	193	282.6	70.7	957.9	711.0
F3W4	30	0.4	193	247.3	106.0	957.9	711.0
F4W4	40	0.4	193	212.0	141.3	957.9	711.0
F0W5	0	0.5	193	386.0	0	957.9	789.2
F1W5	10	0.5	193	347.4	28.2	957.9	789.2
F2W5	20	0.5	193	225.9	56.5	957.9	789.2
F3W5	30	0.5	193	197.6	84.7	957.9	789.2
F4W5	40	0.5	193	169.4	112.9	957.9	789.2

Note: FXWY = X is the replacement percentage x 10, and Y is the w/c ratio percentage x 10

(a)

(b)

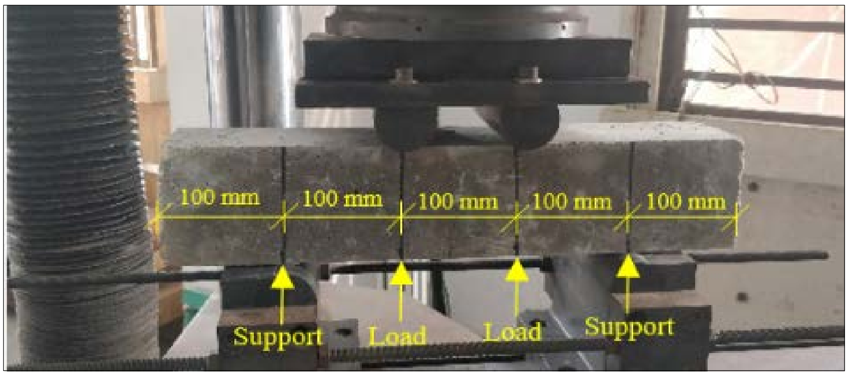

(c)

Figure 3: Test setup: (a) CS and STS tests, (b) CIP test, (c) flexural strength test

B. Density

The average unit weight for different FA contents is illustrated in Figure 6. The value shows that the unit weight decreases with the increase in FA percentage. Thus, concrete becomes lighter as the specific gravity of FA (2.30) is inferior to cement (3.15). It shows that as the w/c ratio increases, the unit weight of the FA blended concrete reduces. These results are consistent with the previous study (Promsawat *et al.*, 2020). Higher water content in concrete results in higher permeable pores. Hence a reduction in unit weight at a hardened state is detected.

Figure 4: Slump test of concrete with w/c ratio of 0.4

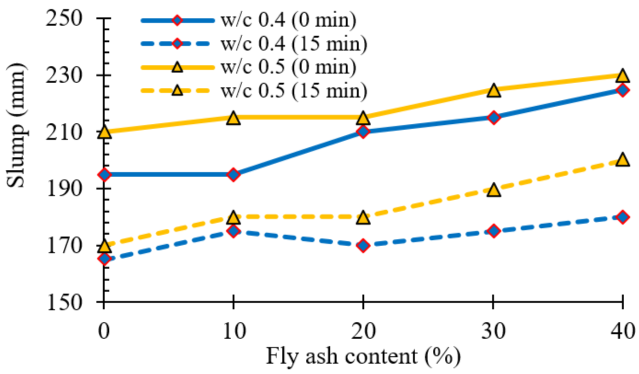

Figure 5: Slump height for different mixes

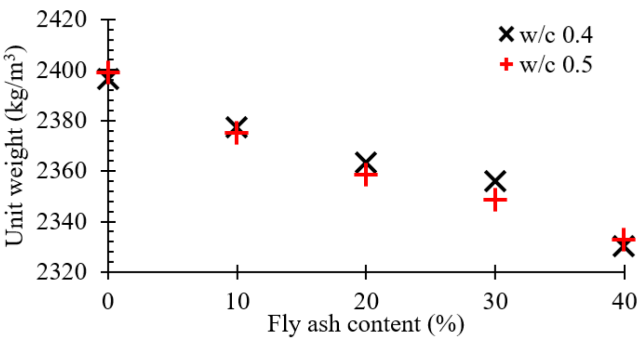

Figure 6: Unit weight for different concrete mixes

C. Compressive Strength

The compressive strength (CS) of cylinders after 7 days, 28 days, and 56 days of curing is shown in Figure 7, which shows the decrement of CS as the FA replacement percentage rises. However, with longer curing time, the increment of CS is higher with FA replacement, which indicates slower strength gain for FA replaced concrete. The increase in CS from 28 days to 56 days age is 13.6% for the control mix (F0W4). On the other hand, it is 24.8%, 64.9%, 37.1%, and 46.7% for 10%, 20%, 30%, and 40% FA respectively and a w/c ratio of 0.4. The combination with 20% FA (F2W4) shows a maximum increase in CS with the curing age. For the w/c ratio of 0.5, a similar scenario is witnessed. The control mix of F0W5 has shown an increase in strength of 6.5% from 28 days to 56 days. In contrast, it is 40.2%, 11.0%, 48.2%, and 73.4%, respectively, for 10%, 20%, 30%, and 40% FA. For this case, the 40% replacement (F4W5) combination shows maximum strength gain with prolonged curing.

Only for the case of F1W4 (w/c ratio of 0.4 and 10% FA replacement) a higher CS is observed in comparison to the reference mix (F0W4). The F1W4 combination has almost equal CS as the control specimen at 28 days. However, at 56 days, strength is higher than control. During the early curing days, the concrete gains strength through cement hydration and forming CH and C-S-H. The pozzolanic reaction of FA is also similar to cement, and the hydration product is closer to C-S-H products. However, the reaction process starts seven or more days after the initial mixing of water for the case of class F FA (Neville, 2016). Hence, with the increase in the curing period, the FA starts to gain strength, and there is a 3% increase in CS for the 10% FA content concrete than the reference concrete without FA after 56 days. The microstructure at 56 days under SEM is shown in Figure 8, where a comparison between F0W4 and F1W4 is presented. It is apparent that the void content efficiently reduces when FA is utilized. A denser C-S-H in F1W4 is also evident, which plays a vital role in improving CS at a later age.

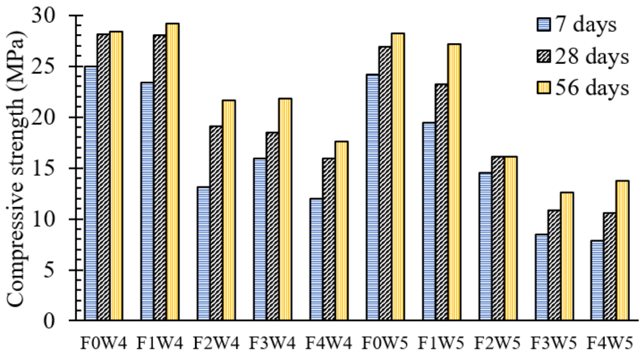

Figure 7: CS of concrete for different percentages of FA replacement

With higher percentages of FA replacement, the rate of strength gain becomes significantly slower, resulting in a lower CS. For a w/c ratio of 0.5, similar type of trend is observed. However, F1W5 (w/c ratio 0.5 and 10% FA replacement) shows only a 3.5% reduction in CS than the control F0W5 at 56 days. In all other cases, with the increase in FA content, a more than 43% decrease is observed in CS. Nonetheless, the increase in the curing period also shows higher CS. In addition, the value of CS increase at 10% replacement is more in w/c ratio 0.4 than 0.5. Furthermore, coarser FA tends to deteriorate the CS of the concrete by slowing down the hydration process and formation of CH and C-S-H (Moghaddam *et al.*, 2019). Therefore, the coarser FA used in this study shows a lesser strength gain at an early age, especially with higher water content in the concrete.

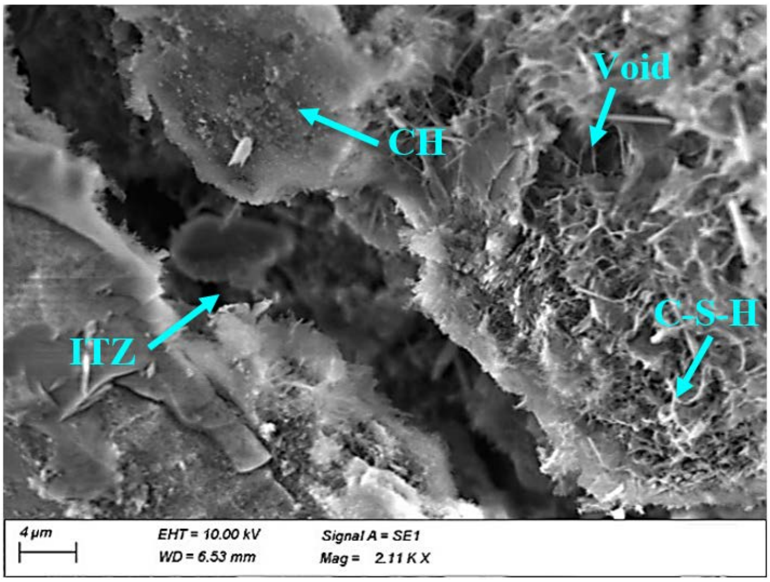

(a)

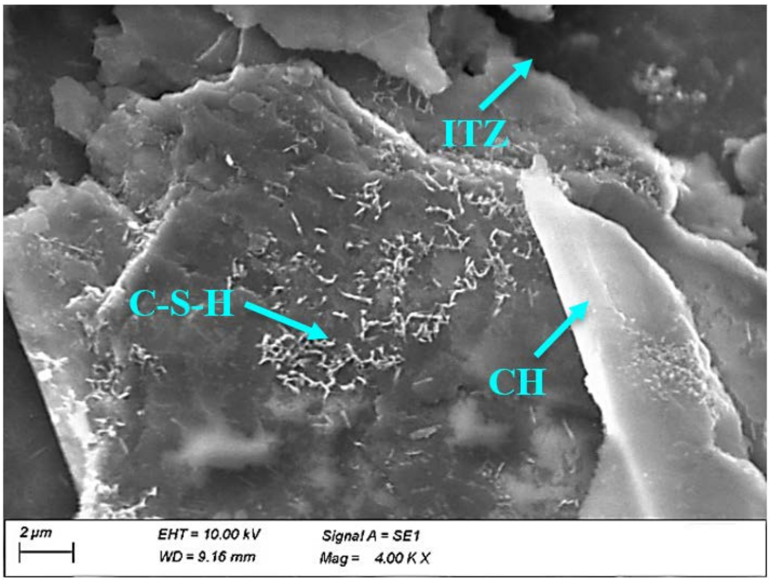

(b)

Figure 8: Microstructure of concrete under SEM (a) F0W4 (b) F1W4

D. Modulus of Elasticity

Young's modulus (YM) for different FA replacements is shown in Figure 9. At 10% replacement, the YM reduces by 7% and increases by 3% after curing for 7 and 28 days, respectively, at a w/c ratio of 0.4. With the increase of FA replacement, the YM decreases after 20% replacement. At 40% LSP replacement, the reduction is 53% and 32% at 7 and 28 days, respectively. For the w/c ratio of 0.5, the YM deteriorated with increasing FA content after 7 days and 28 days of curing. The reduction varies from 14 – 49% at 7 days and 17 – 40% at 28 days. Therefore, except for one case of a 10% FA replacement, the YM decreases with the increase in FA content. These results are consistent with the strength gain of FA replaced concrete with the age and FA percentages.

E. Rupture Strain

Rupture strain (RS) for different percentages of FA replacements is shown in Figure 10. The RS for a w/c of 0.4 shows closer values after 7 days and 28 days of age, and values vary between 0.00196 and 0.00256. There are no significant changes in RS with the increment of FA replacements. However, for a w/c ratio of 0.5, the RS increases with higher FA content in concrete. At 28 days, RS increases from 0.00382 to 0.00529, with the maximum at 40% FA replaced concrete. Higher FA replacement indicates lower strength and better ductility. With a decrease in CS, RS increases more than two times for a w/c of 0.5 than a w/c of 0.4.

F. Toughness

Rupture Toughness for different FA replacements is shown `in Figure 11. It depicts the reduction of toughness with the increase of FA percentage after 7 and 28 days of curing for the w/c ratio of 0.4. Especially for 40% FA replaced concrete, the reduction in toughness is significantly high at 69.6%. However, for the w/c ratio of 0.5 at 28 days, toughness is higher with FA replacement, except for the case of 10% replacement. The maximum toughness was found at 30% replacement with an increment of 19%. It is evident from the test result that lower-strength concrete is more ductile. The increase in toughness results in an upturn in the plastic zone of the stress-strain diagram (Figure 16).

G. Splitting Tensile Strength

The splitting tensile strength (STS) falls with the increase of FA replacement which is given in Figure 12. For the w/c ratio of 0.4, at 40% replacement, the subsidence of strength is 21.7%. However, F1W4 shows only a 1.4% decrease in strength during the 56 days curing period. Similar to the strength gain for CS, STS gain from 7 days to 56 days is significantly higher with FA replaced concrete. Compared to the 13.2% for the control after 56 days, strength gain is 29.5%, 28.6%, 31%, and 46.9% for the 10%, 20%, 30%, and 40% FA concrete, respectively. A gradual drop in strength is also observed with the increase in FA content for the w/c ratio of 0.5. The tensile strength decreases almost linearly up to 26.7% for F4W5. At this w/c ratio, F1W5 with the replacement of 10% FA gives better results than others. It shows the slightest decrease in strength of 3.3% compared to F0W5 with no FA. Like before, at the w/c ratio of 0.5, STS gain from 7 days to 56 days is 38.1%, 28.3%, 83.3%, and 83.3% for 10 – 40 % FA replaced concrete compared to the STS gain of 15.4% for the control specimen.

H. Chloride Ion Penetrability

Concrete surface resistivity is examined through the Resipod surface resistivity meter in compliance with AASHTO TP 95 (2014). These data can be compared with the chloride ion penetrability (CIP) indicators following the AASHTO TP 95 (2014), where the CIP level varies between high to negligible. The lowest surface resistivity value indicates the highest CIP. These values can be correlated to values suggested by ASTM C1202 (2021). For example, surface resistivity less than 12 kΩ-cm, equivalent to 4000+ Coulombs, is classified as high CIP. Whereas values in the range of 12-21 kΩ-cm (2000 – 4000 Coulombs), 21-27 kΩ-cm (1000 – 2000 Coulombs), and 37-254 kΩ-cm (100 – 1000 Coulombs) are categorized respectively as moderate, low, and very low CIP.

A surface resistivity value higher than 254 kΩ-cm (less than 100 Coulombs) is considered negligible CIP. The surface resistivity after a curing period of 7 days, 28 days, and 56 days is measured, and the result is presented in Figure 13. Figure 13 shows that the CIP declines with the increase in FA after 28 days and 56 days of curing, especially with the w/c ratio of 0.4. Increased resistance to CIP is brought on by improved pore structure and a drop in permeability induced by FA (Thomas *et al.*, 2017). The penetrability deteriorates with the rise in FA replacement level. In almost all cases, the penetrability is high. Only at F3W4 and F4W4 the penetrability is moderate. For the w/c ratio of 0.5, the CIP decreases with FA replaced concrete. After 56 days, the CIP is lower for all FA concrete than the control one. However, the surface resistivity value remains unchanged for FA concrete due to higher void content at a higher w/c ratio. Thus, the increase in FA replacement and curing period will reduce the CIP; however, the reduction is higher for a lower w/c ratio.

I. Shrinkage of Concrete Beam

Shrinkage of the 100 x 100 x 500 mm concrete beams is measured at 35 days using a length comparator. The shrinkage percentage is shown in Figure 14. As the figure shows, shrinkage is maximum for the control concrete for the w/c ratios of 0.4 and 0.5. There is a distinct drop in shrinkage for w/c ratio 0.4, where reduction varies between 48.5% and 82.4%, with a maximum drop for the 40% FA replaced concrete. For the w/c ratio of 0.5, the reduction in shrinkage varied between 10.5% and 36.8%, with the lowest for the 10% FA replaced concrete. The hydration process of FA replaced concrete is slower than the OPC, resulting in lesser shrinkage of the FA replaced concrete (Liu *et al.*, 2022). Control concrete of F0W4 has the highest cement content, giving higher hydration. Hence it has the highest shrinkage. With a higher w/c ratio, the hydration process is relatively slow because of the lower amount of cement. Hence it shows relatively lower shrinkage.

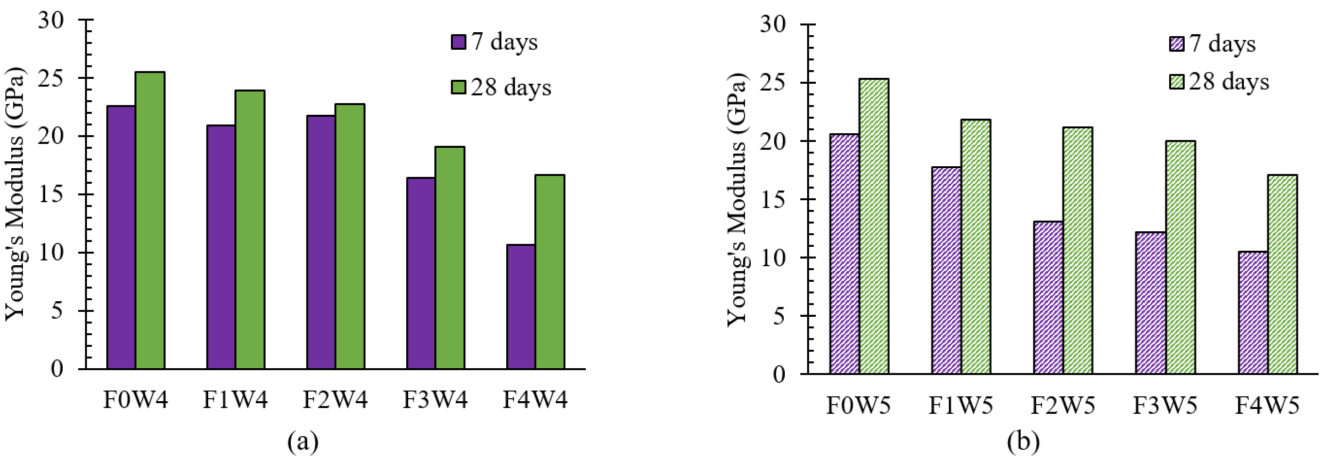

Figure 9: Young's modulus for (a) w/c ratio 0.4 (b) w/c ratio 0.5

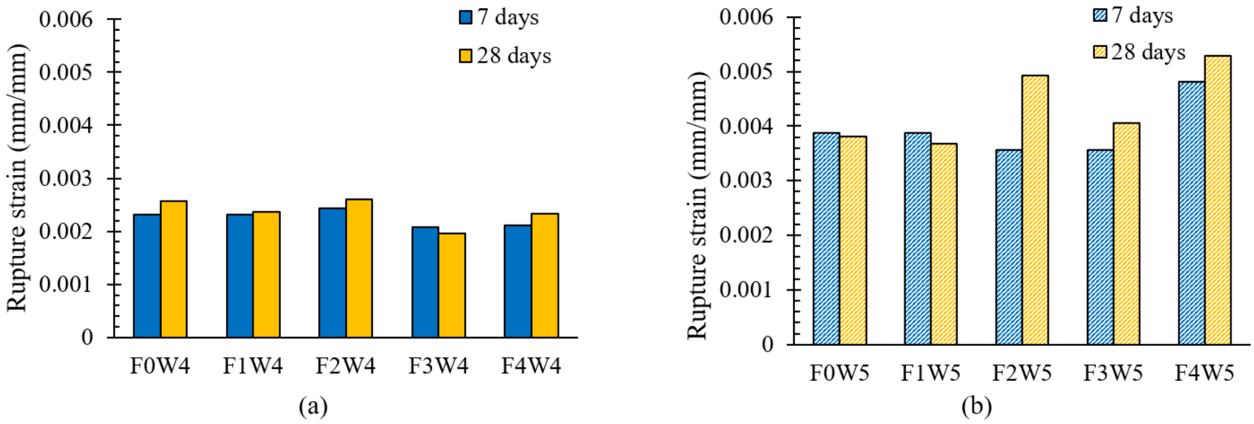

Figure 10: Rupture strain for (a) w/c ratio 0.4 (b) w/c ratio 0.5

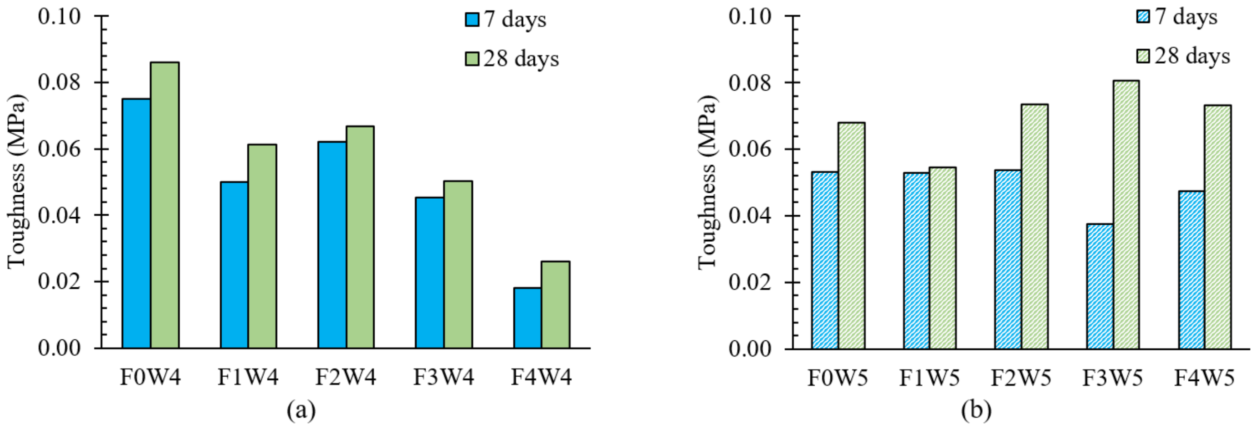

Figure 11: Toughness for (a) w/c ratio 0.4 (b) w/c ratio 0.5

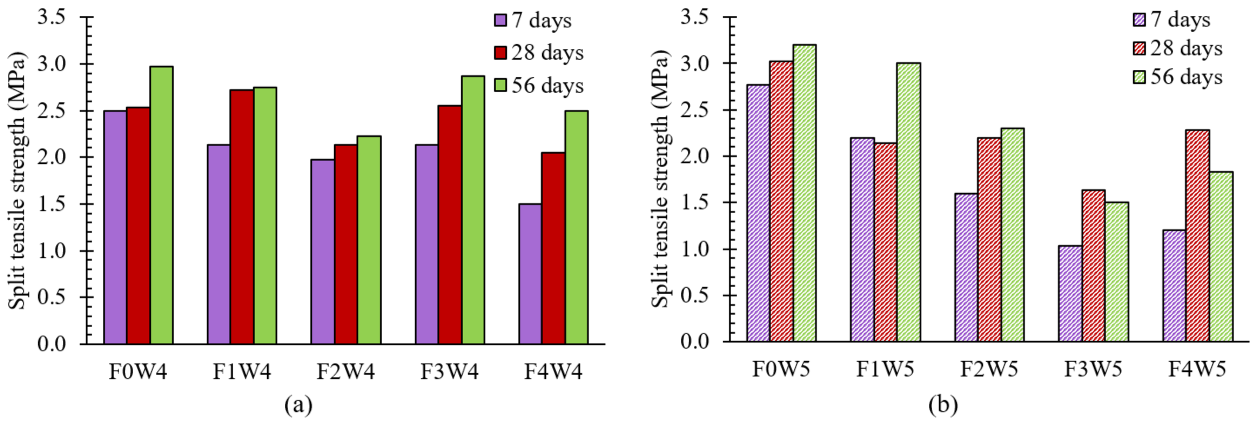

Figure 12: STS of concrete over the age (a) w/c ratio 0.4 (b) w/c ratio 0.5

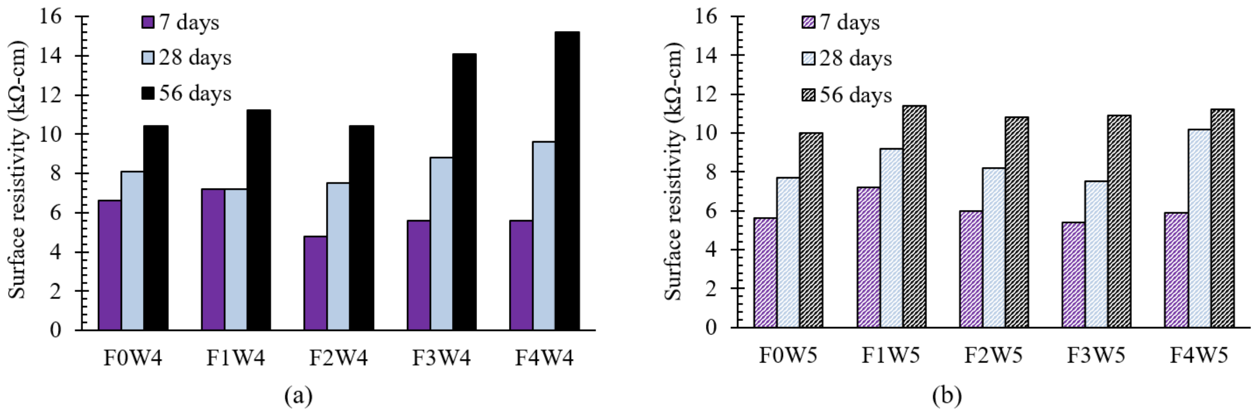

Figure 13: Surface resistivity for (a) w/c ratio 0.4 (b) w/c ratio 0.5

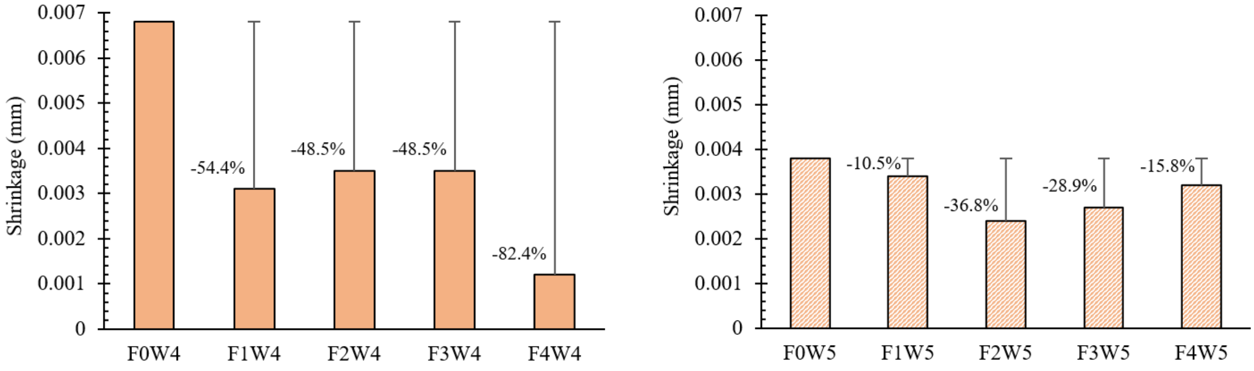

(a) (b)

Figure 14: Shrinkage for (a) w/c ratio 0.4; (b) w/c ratio 0.5

J. Flexural Strength of Beam

Figure 15 illustrates concrete beams' flexural strength (FS) for different FA replacement percentages at 56 days after casting. It shows the reduction of FS with the replacement of FA. For the w/c ratio 0.4, the strength reduces almost linearly from 8% to 29%, except for the case of F3W4, where the reduction is only 4.8%. For the w/c ratio 0.5, a 10% increase in FS is observed for F1W5 with 10% FA replacement. However, with higher FA percentages, FS decreases up to 40.3%. This trend is almost similar to the other mechanical properties observed in this study. Slow hydration of FA and coarser size of FA cause a drop in FS of FA contained concrete. However, up to 10% FA replacement can be considered, especially for lower strength concrete at higher w/c ratios. Figure 16 shows the stress-strain plot for different replacements of FA at both the w/c ratios of 0.4 and 0.5. The figures show that maximum strain is higher for a higher-strength concrete with a lesser w/c ratio. Furthermore, the failure pattern is similar for both w/c ratios. Except for F1W5, failure strain and stress are reduced with the increasing FA replacement. At the w/c ratio of 0.5, the maximum stress decreases rapidly with higher FA content. Furthermore, the stress-strain curve gets steeper. The toughness of the concrete has also been measured from the stress-strain plots and depicted in Figure 17. With the higher strength concrete, toughness reduces with the increasing FA replacement, and the reduction is maximum for 40% replacement. The decrease is relatively less in the case of lower strength concrete with the w/c ratio of 0.5. With combinations of F1W5 and F3W5, there is even an increase in toughness.

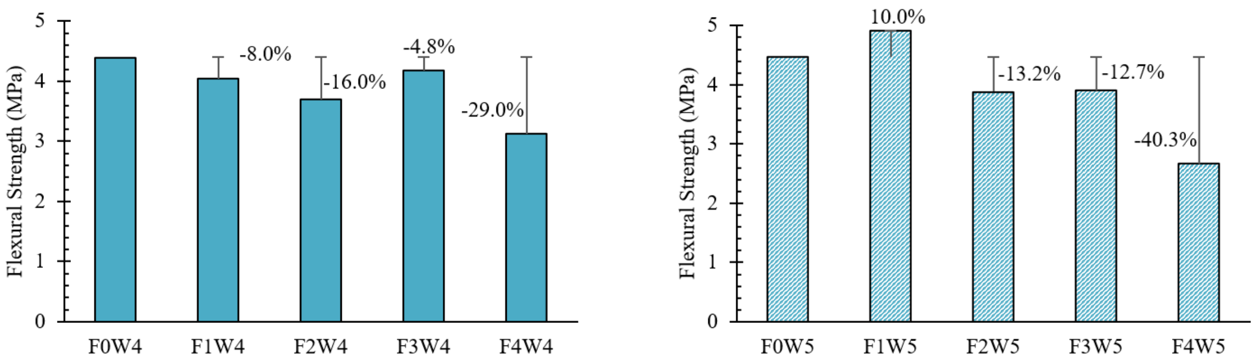

(a) (b)

Figure 15: Flexural strength for (a) w/c ratio 0.4 (b) w/c ratio 0.5

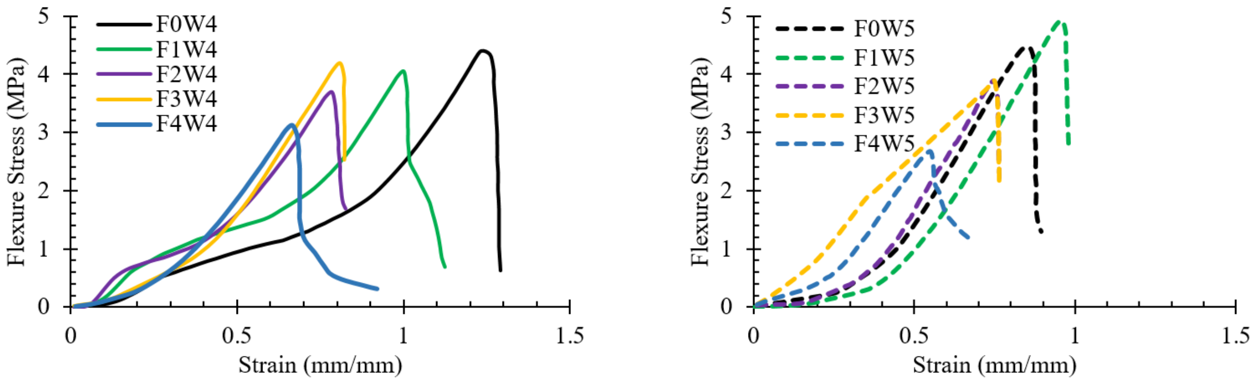

(a) (b)

Figure 16: Stress vs. strain plot for (a) w/c ratio 0.4 (b) w/c ratio 0.5

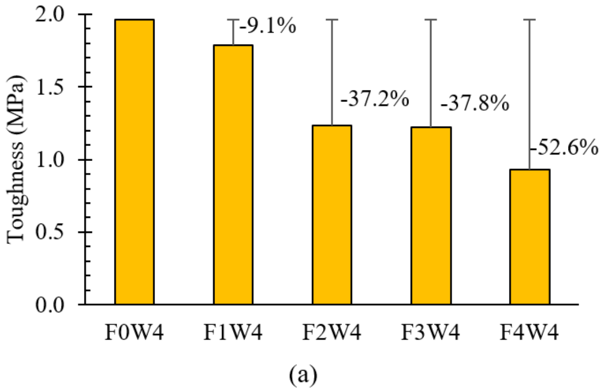

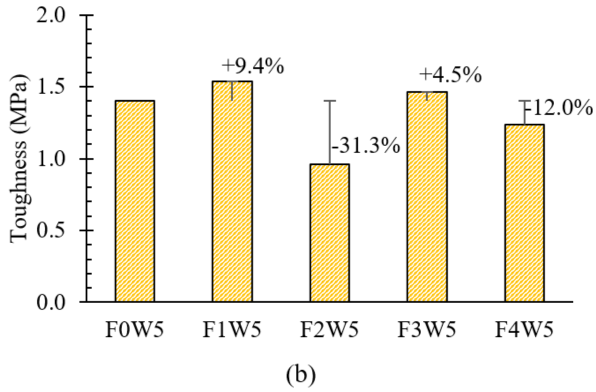

Figure 17: Toughness comparison (a) w/c ratio 0.4 (b) w/c ratio 0.5

K. Comparison of Mechanical Properties

Several codes provide expressions to determine the STS, YM, and FS of concrete, such as ACI 318-14 (2014), AS 3600 (2009), fib 2010 (2010), Eurocode 2 (2005), CSA A23.3-14 (2014), ACI 363R (2010) as given in Table 5. As observed from Table 5, code prediction for STS and FS are affined to the CS. Hence, two equations are proposed for the STS and FS in Equations 5 and 15 with an R squared value of 0.994 and 0.987, respectively. ACI 318-14 (2014) and CSA A23.3-14 (2014) indicate that YM is linked to the density and CS of concrete. With increasing FA percentages, FA incorporated concrete has a lower unit weight, CS, and YM. However, none of the equations considered the effect of FA in concrete. Therefore, an equation is proposed using a multiple regression model for YM where the effect of unit weight, CS and FA content is considered and shown in Equation 10.

The STS, YM, and FS calculated using the equations suggested by the codes and the equation proposed in this study are compared in Figure 18, Figure 19, and Figure 20, respectively. Here, equations are suggested depending on the experimental results of STS and YM at 28 days and FS at 56 days. ACI 318-14 (2014) and the proposed equations for the STS are almost similar and overestimate the STS data at lower w/c ratio and FA replacement percentages, as displayed in Figure 18. However, these equations underestimate the STS by as much as 17% for higher w/c ratio and FA contents. Fib (2010) and Eurocode 2 (2005) provide the best correlation, especially at the w/c ratio of 0.4. For the w/c ratio of 0.5, the equations mentioned in these codes underestimate the STS by up to 32%. AS 3600 (2009), significantly underestimates the STS values in all the cases. For the YM equations, the proposed equation, ACI 318-14 (2014), AS 3600 (2009), and CSA A23.3-14 (2014), provide similar predictions with a relatively smaller variation, as illustrated in Figure 19. However, fib (2010) significantly overestimates the YM values with variation as high as 51%. The proposed equation for the calculation of FS gives a good prediction. However, the variation is a maximum of 23% for the w/c ratio of 0.5. A similar prediction is noted for the code equation of fib (2010). On the contrary, ACI 318-14 (2014) and CSA A23.3-14 (2014) underestimate the FS data by 17 – 45%. The FS data are also compared with the ACI 363R, which showed that ACI 363R overestimates the data by 0 – 30%.

Table 5
Equations for calculating STS, YM, and FS

Splitting tensile strength, STS (MPa)	ACI 318-14 (2014)	$STS = 0.556\sqrt{f_{cm}}$	(1)
	AS 3600 (2009)	$STS = 0.36\sqrt{f_{cm}}$	(2)
	fib (2010)	$STS = 0.3(f_{cm})^{2/3}$	(3)
	Eurocode 2 (2005)	$STS = 0.556\alpha_s\sqrt{f_{cm}}$	(4)
	Proposed Eqn.	$STS = 0.546\sqrt{f_{cm}}$; $R^2 = 0.994$	(5)
Young's modulus, YM (MPa)	ACI 318-14 (2014)	$YM = w_c^{1.5}\, 0.043\sqrt{f_{cm}}$	(6)
	AS 3600 (2009)	$YM = 5055\sqrt{0.9f_{cm}}$ (for $f_{cm} < 40$ MPa)	(7)
	fib (2010)	$YM = E_0\, \alpha_E\, (f_{cm}/10)^{1/3}$	(8)
	CSA A23.3-14 (2014)	$YM = (3300\sqrt{f_{cm}} + 6900)\,(w_c/2300)^{1.5}$	(9)
	Proposed Eqn.	$YM = w_c^{1.5} 0.040\sqrt{f_{cm}} + 27.43FA$; $R^2 = 0.991$	(10)
Flexural strength, FS (MPa)	ACI 318-14 (2014)	$FS = 0.62\sqrt{f_{cm}}$	(11)
	ACI 363R (2010)	$FS = 0.94\sqrt{f_{cm}}$	(12)
	fib (2010)	$FS = 0.3\ \frac{f_{cm}^{2/3}}{\alpha_f}$	(13)
	CSA A23.3-14 (2014)	$FS = 0.6\lambda\sqrt{f_{cm}}$	(14)
	Proposed Eqn.	$FS = 0.849\sqrt{f_{cm}}$; $R^2 = 0.987$	(15)

Where, f_{cm} = CS (MPa), STS = splitting tensile strength (MPa), YM = Young's modulus, FS = flexural strength (MPa), w_c = density of concrete, FA = fly ash content (%), α_s = 0.9, E_0 α_E = 21500 MPa, $\alpha_f = \frac{0.06h^{0.7}}{1+0.06h^{0.7}}$, h = depth of beam (mm), λ = 1.0 for regular density concrete.

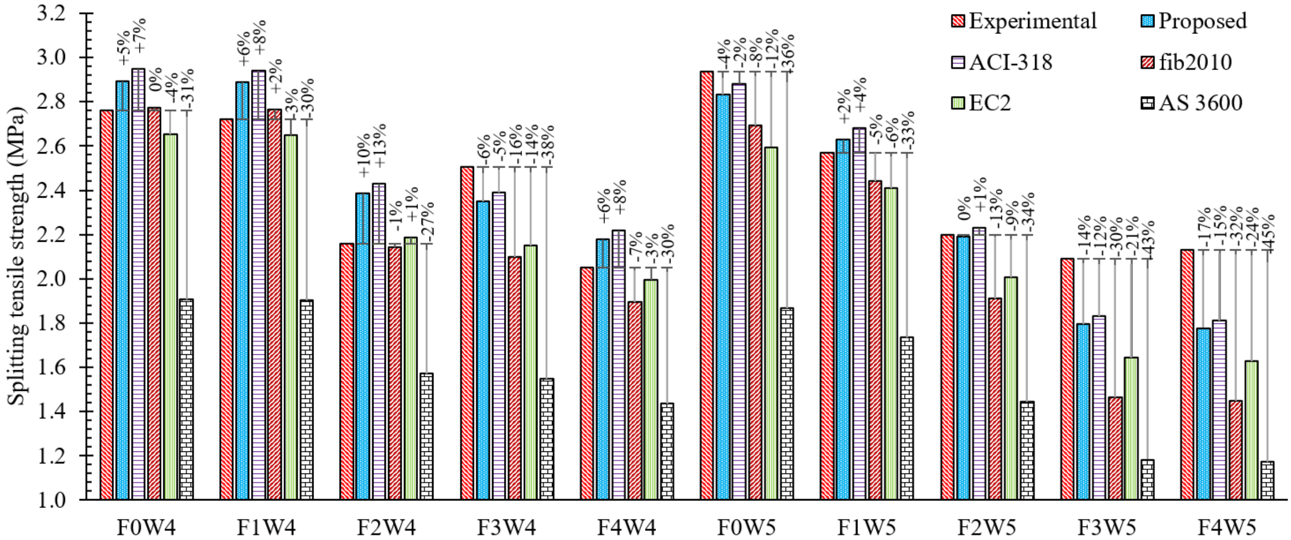

Figure 18: Percentage variation of proposed STS equation with codes prediction

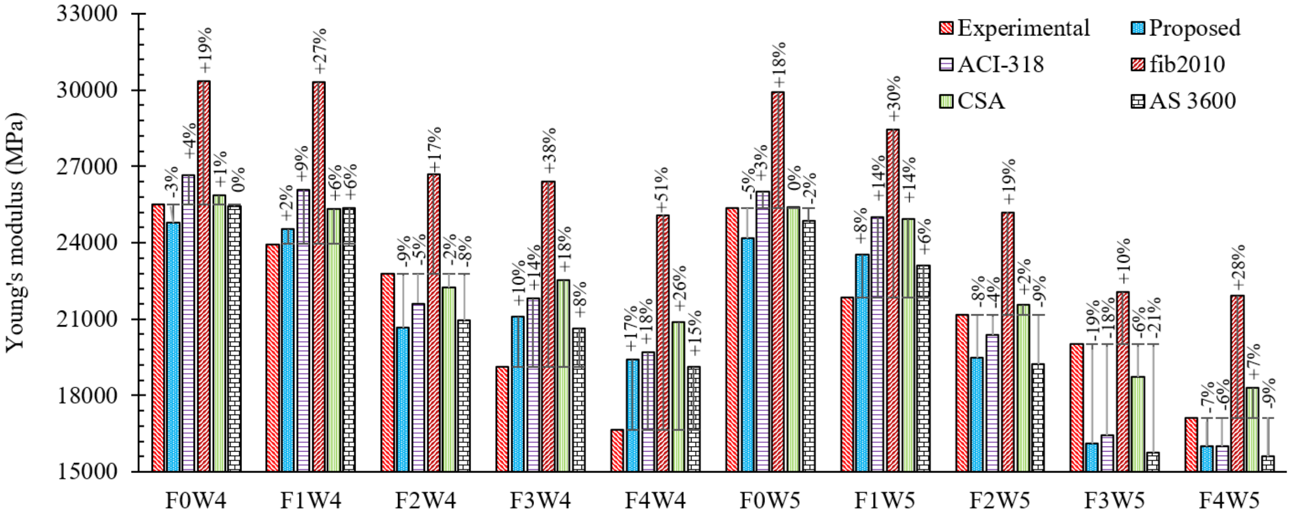

Figure 19: Percentage variation of proposed YM equation with codes prediction

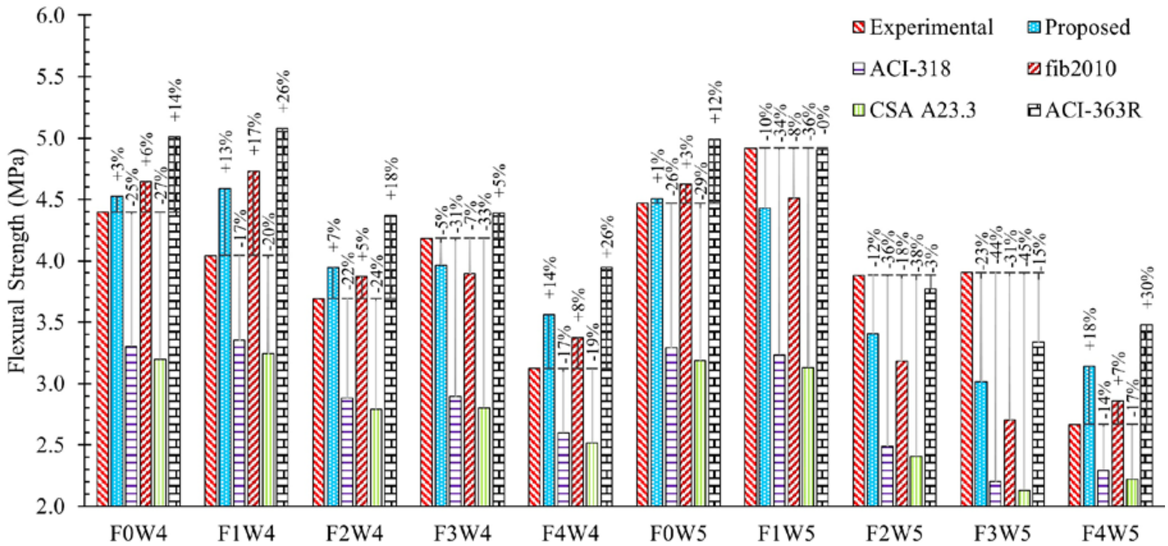

Figure 20: Percentage variation of proposed FS equation with codes prediction

9. CONCLUSIONS

This study explored the feasibility of FA as a partial replacement of cement in concrete and disclosed that the replacement of fly ash reduces strength in concrete. However, with a higher curing period, the change in strength is insignificant in the case of a lower percentage of replacement. From the analysis of the test results following findings are identified:

i. The workability of concrete escalates with the increase in FA replacement. The maximum workability is observed at 40% FA replacement both immediately after the casting and after 15 minutes. The increase in a slump is a maximum of 15% for the w/c ratio of 0.4 immediately after concrete casting.

ii. The density of concrete diminishes linearly with higher FA replacement. However, density only decreases by 3% for a 40% FA interchange.

iii. The CS of FA concrete shows 11% to 73% strength gain with age from 28 days to 56 days. This is especially significant for higher FA substitution. Generally, CS reduces with the increase in FA replacement. The lowest CS is found at 40% FA replacement. However, 10% FA replaced concrete shows promising results after 56 days curing period. For the w/c ratio of 0.4, the CS does not reduce rather increases by 3% from the control specimen. Whereas, for the 0.5 w/c ratio, the reduction in CS is only 3.5% on 56 days.

iv. Like the CS, YM for FA replaced concrete also shows a constant decrease up to 32%, and 40% for w/c ratios of 0.4 and 0.5, respectively, at 28 days. Coarser FA slows the hydration procedure causing a slower gain in strength.

v. The rupture strain did not demonstrate substantial change with the FA replacement for the w/c ratio of 0.4. However, for the w/c ratio of 0.5, it increases and gives the maximum result at 40% FA replacement, which, after 28 days, is 38.7% greater than the reference concrete.

vi. The toughness of concrete decreases with the replacement of FA for the w/c ratio of 0.4. At 40% FA replacement, the reduction is 69.6%. However, it improves for the w/c ratio of 0.5. For the w/c ratio of 0.5, 30% FA replacement gives 19% higher toughness than the control specimen.

vii. The STS reduces with the increase of FA replacement and up to 21.7% and 26.7% strength drop is observed for w/c ratios of 0.4 and 0.5, respectively. The reduction is minimum at 10% replacement and only 1.4% and 3.3%, respectively compared to the control specimen. Furthermore, FA concrete shows up to 83.3% STS gain from 7 days to 56 days of concrete age.

viii. CIP decreases with the increase in FA replacement. The reduction is a maximum at 40% FA substitution. At 30 and 40% FA substitution with the w/c ratio of 0.4, CIP is moderate, while in all other cases, it is highly penetrable.

ix. Shrinkage reduces rapidly with the increase in FA replacement. The maximum reduction is 82.4% and 36.8% at 40% and 20% FA levels, respectively, for w/c ratios 0.4 and 0.5 compared to the control concrete.

x. The FS reduces with the substitution of FA in concrete. The reduction is 16% for up to 30% FA substitution. For the combination of F1W5, a 10% increase in FS is observed compared to the control concrete. However, for 40% FA concrete drop in FS is 29.0% and 40.3% for w/c ratios of 0.4 and 0.5, respectively. The toughness was measured from the load-deflection plots of beam tests; comparable values are observed at 10% FA concrete for both w/c ratios.

xi. Three equations are proposed to predict the STS, YM, and FS from the CS, unit weight, and FA of concrete based on the experimental data collected in this study. The values generated from these equations are then compared with the experimental data and several code-predicted data. Although several codes provided good correlation, not a single code gives consistently good correlation to predict these properties. Hence, a revision of code equations may be considered.

Concrete with FA shows superior concrete durability characteristics in terms of shrinkage and chloride ion penetrability. However, a higher percentage of FA substitution results in lower mechanical properties. Hence, up to 10% FA replacement with a higher curing period may be suitable for producing environment-friendly concrete.

ACKNOWLEDGEMENTS

This study has been conducted at the Concrete Lab of the Civil Engineering Department, MIST, Dhaka, Bangladesh. A special thank goes to the laboratory staff and the Head of the Department of Civil Engineering.

REFERENCES

AASHTO TP 95. (2014). Standard Method of Test for Surface Resistivity Indication of Concrete’s Ability to Resist Chloride Ion Penetration. *AASHTO Annual Meeting, Orlando, FL*.

ACI 116R. (2000). Cement and Concrete Terminology. *American Concrete Institute, Farmington Hills, MI*.

ACI 211.1-91. (1994). Standard Practice of Selecting Proportions for Normal, Heavy-weight, and Mass Concrete. *American Concrete Institute, Farmington Hills, MI*.

ACI 225R. (2016). Guide to the Selection and Use of Hydraulic Cements *American Concrete Institute, Farmington Hills, MI*.

ACI 318-14. (2014). Building Code Requirements for Structural Concrete and Commentary. *American Concrete Institute, Farmington Hills, MI*.

ACI 363R. (2010). Report on High-Strength Concrete. *American Concrete Institute, Farmington Hills, MI*.

Ahmaruzzaman, M. (2010). A review on the utilization of fly ash. *Progress in Energy and Combustion Science, 36*(3), 327-363. doi:https://doi.org/10.1016/j.pecs.2009.11.003

Amiri, A., Olfati, A., Najjar, S., Beiranvand, P., & Fard, M. H. (2016). THE EFFECT OF FLY ASH ON FLEXURAL CAPACITY CONCRETE BEAMS. *Advances in Science and Technology Research Journal, 10*, 89-95. doi:10.12913/22998624/62630

Andrew, R. (2018). Global CO₂ Emissions from Cement Production. *Earth System Science Data Discussions*, 1-61. doi:10.5194/essd-2018-90

AS 3600. (2009). Concrete Structures: Design Properties of materials. *Australian Standard, Australia*.

ASTM C29. (2021). Standard Test Method for Bulk Density ("Unit Weight") and Voids in Aggregate. *ASTM International, West Conshohocken, PA*.

ASTM C33. (2018). Standard Specification for Concrete Aggregates. *ASTM International, West Conshohocken, PA*.

ASTM C78. (2022). Standard Test Method for Flexural Strength of Concrete (Using Simple Beam with Third-Point Loading). *ASTM International, West Conshohocken, PA*.

ASTM C109. (2020). Standard Test Method for Compressive Strength of Hydraulic Cement Mortars (Using 2-in. or [50-mm] Cube Specimens). *ASTM International, West Conshohocken, PA*.

ASTM C127. (2015). Standard Test Method for Relative Density (Specific Gravity) and Absorption of Coarse Aggregate. *ASTM International, West Conshohocken, PA*.

ASTM C128. (2015). Standard Test Method for Relative Density (Specific Gravity) and Absorption of Fine Aggregate. *ASTM International, West Conshohocken, PA*.

ASTM C136. (2014). Standard Test Method for Sieve Analysis of Fine and Coarse Aggregates. *ASTM International, West Conshohocken, PA*.

ASTM C150. (2021). Standard Specification for Portland Cement. *ASTM International, West Conshohocken, PA*.

ASTM C187. (2016). Standard Test Method for Amount of Water Required for Normal Consistency of Hydraulic Cement Paste. *ASTM International, West Conshohocken, PA*.

ASTM C188. (2017). Standard Test Method for Density of Hydraulic Cement. *ASTM International, West Conshohocken, PA*.

ASTM C191. (2021). Standard Test Methods for Time of Setting of Hydraulic Cement by Vicat Needle. *ASTM International, West Conshohocken, PA*.

ASTM C618. (2019). Standard Specification for Coal Fly Ash and Raw or Calcined Natural Pozzolan for Use in Concrete. *ASTM International, West Conshohocken, PA*.

ASTM C1202. (2021). Standard Test Method for Electrical Indication of Concrete's Ability to Resist Chloride Ion Penetration. *ASTM International, West Conshohocken, PA*.

Babor, D., Plian, D., & Judele, L. (2009). Environmental Impact of Concrete. *Bulletin of the Polytechnic Institute of Jassy, CONSTRUCTIONS. ARCHITECTURE Section, Tomme LV (LIX), Fascicle 4, pages 27-36 (2009), LV (LIX)*.

Barcelo, L., Kline, J., Walenta, G., & Gartner, E. (2014). Cement and carbon emissions. *Materials and Structures, 47*(6), 1055-1065. doi:10.1617/s11527-013-0114-5

Breeze, P. (2015). Chapter 1 - An Introduction to Coal-Fired Power Generation. In P. Breeze (Ed.), *Coal-Fired Generation* (pp. 1-7). Boston: Academic Press.

Chindaprasirt, P., Homwuttiwong, S., & Sirivivatnanon, V. (2004). Influence of fly ash fineness on strength, drying shrinkage and sulfate resistance of blended cement mortar. *Cement and Concrete Research, 34*(7), 1087-1092. doi:https://doi.org/10.1016/j.cemconres.2003.11.021

Chindasiriphan, P., Yokota, H., & Pimpakan, P. (2020). Effect of fly ash and superabsorbent polymer on concrete self-healing ability. *Construction and Building Materials, 233*, 116975. doi:10.1016/j.conbuildmat.2019.116975

Chinh, N. (2021). Flexural performance of reinforced concrete beams made with locally sourced fly ash. *Journal of Science and Technology in Civil Engineering (STCE) - NUCE, 15*, 38-50. doi:10.31814/stce.nuce2021-15(2)-04

CSA A23.3-14. (2014). Design of Concrete Structures. *Canadian Standards Association, Canada*.

Eurocode 2. (2005). EN 1992-1-1, Design of Concrete Structures – Part 1–1: General Rules and Rules for Buildings. *Thomas Telford, London, UK*.

Fantu, T., Alemayehu, G., Kebede, G., Abebe, Y., Selvaraj, S. K., & P, V. (2021). Experimental investigation of compressive strength for fly ash on high strength concrete C-55 grade. *Materials Today: Proceedings, 46*. doi:10.1016/j.matpr.2021.01.213

Feiz, R., Ammenberg, J., Baas, L., Eklund, M., Helgstrand, A., & Marshall, R. (2015). Improving the CO2 performance of cement, part II: framework for assessing CO2 improvement measures in the cement industry. *Journal of Cleaner Production, 98*, 282-291. doi:https://doi.org/10.1016/j.jclepro.2014.01.103

fib 2010. (2010). fib Model Code for Concrete Structures. *International Fedaration for Structural Concrete*.

fib. (2010). fib Model Code for Concrete Structures. *International Fedaration for Structural Concrete*.

Fuzail Hashmi, A., Shariq, M., & Baqi, A. (2020). Flexural performance of high volume fly ash reinforced concrete beams and slabs. *Structures, 25*, 868-880. doi:https://doi.org/10.1016/j.istruc.2020.03.071

Golewski, G. L. (2018). Green concrete composite incorporating fly ash with high strength and fracture toughness. *Journal of Cleaner Production, 172*, 218-226. doi:https://doi.org/10.1016/j.jclepro.2017.10.065

Hardjito, D., Wallah, S. E., Sumajouw, D. M. J., & Rangan, B. V. J. A. M. J. (2004). ON THE DEVELOPMENT OF FLY ASH-BASED GEOPOLYMER CONCRETE. *ACI Materials Journal, 101*, 467-472.

Howladar, M. F., & Islam, M. R. (2016). A study on physico-chemical properties and uses of coal ash of Barapukuria Coal Fired Thermal Power Plant, Dinajpur, for environmental sustainability. *Energy, Ecology and Environment, 1*(4), 233-247. doi:10.1007/s40974-016-0022-y

Islam, M. J., Ahmed, T., Imam, S. M. F. B., Ifaz, M., & Islam, H. (2022). Flexural and impact behavior of textile reinforced concrete panel. *International Journal of Protective Structures*, 20414196221095250. doi:10.1177/20414196221095250

Islam, M. J., Borsha, N. T., Meghna, N. N., & Enam, R. B.-t. (2023, 2023//). *Mechanical and Durability Properties of Fly Ash Blended Concrete with Gi Fiber.* Paper presented at the Proceedings of the Canadian Society of Civil Engineering Annual Conference 2021, Singapore.

Jamora, J. B., Gudia, S. E. L., Go, A. W., Giduquio, M. B., & Loretero, M. E. (2020). Potential CO2 reduction and cost evaluation in use and transport of coal ash as cement replacement: A case in the Philippines. *Waste Management, 103*, 137-145. doi:https://doi.org/10.1016/j.wasman.2019.12.026

Jiang, D., Li, X., Lv, Y., Zhou, M., He, C., Jiang, W., Liu, Z., & Li, C. (2020). Utilization of limestone powder and fly ash in blended cement: Rheology, strength and hydration characteristics. *Construction and Building Materials, 232*, 117228. doi:https://doi.org/10.1016/j.conbuildmat.2019.117228

Jiménez-Quero, V. G., León-Martínez, F. M., Montes-García, P., Gaona-Tiburcio, C., & Chacón-Nava, J. G. (2013). Influence of sugar-cane bagasse ash and fly ash on the rheological behavior of cement pastes and mortars. *Construction and Building Materials, 40*, 691-701. doi:https://doi.org/10.1016/j.conbuildmat.2012.11.023

Joanna, P. S., Parvati, T. S., Rooby, J., & Preetha, R. (2020). A study on the flexural behavior of sustainable concrete beams with high volume fly ash. *Materials Today: Proceedings, 33*, 1149-1157. doi:https://doi.org/10.1016/j.matpr.2020.07.343

Khan, M. D. I., Abdy Sayyed, M. A., Yadav, G. S., & Varma, S. H. (2021). The impact of fly ash and structural fiber on the mechanical properties of concrete. *Materials Today:*

Proceedings, 39, 508-512. doi:https://doi.org/10.1016/j.matpr.2020.08.242

Khongpermgoson, P., Boonlao, K., Ananthanet, N., Thitithananon, T., Jaturapitakkul, C., Tangchirapat, W., & Ban, C. C. (2020). The mechanical properties and heat development behavior of high strength concrete containing high fineness coal bottom ash as a pozzolanic binder. *Construction and Building Materials, 253*, 119239. doi:https://doi.org/10.1016/j.conbuildmat.2020.119239

Koodalloor Parasuraman, R., Siddik, M., & Nazeer, M. (2011). *WORKABILITY AND STRENGTH STUDIES ON FLY ASH MODIFIED MASONRY MORTARS*.

Lanzerstorfer, C. (2018). Fly ash from coal combustion: Dependence of the concentration of various elements on the particle size. *Fuel, 228*, 263-271. doi:10.1016/j.fuel.2018.04.136

Laxman Kudva, P., Nayak, G., Shetty, K. K., & Sugandhini, H. K. (2022). A sustainable approach to designing high volume fly ash concretes. *Materials Today: Proceedings*. doi:https://doi.org/10.1016/j.matpr.2022.04.165

Liu, Z., Takasu, K., Koyamada, H., & Suyama, H. (2022). A study on engineering properties and environmental impact of sustainable concrete with fly ash or GGBS. *Construction and Building Materials, 316*, 125776. doi:https://doi.org/10.1016/j.conbuildmat.2021.125776

Moghaddam, F., Sirivivatnanon, V., & Vessalas, K. (2019). The effect of fly ash fineness on heat of hydration, microstructure, flow and compressive strength of blended cement pastes. *Case Studies in Construction Materials, 10*, e00218. doi:10.1016/j.cscm.2019.e00218

Nath, P., & Sarker, P. (2011). Effect of Fly Ash on the Durability Properties of High Strength Concrete. *Procedia Engineering, 14*, 1149-1156. doi:https://doi.org/10.1016/j.proeng.2011.07.144

Neville, A. M. (2016). *Properties of Concrete* (Fifth ed.): Pearson.

Oner, A., Akyuz, S., & Yildiz, R. (2005). An experimental study on strength development of concrete containing fly ash and optimum usage of fly ash in concrete. *Cement and Concrete Research, 35*(6), 1165-1171. doi:https://doi.org/10.1016/j.cemconres.2004.09.031

Promsawat, P., Chatveera, B., Sua-iam, G., & Makul, N. (2020). Properties of self-compacting concrete prepared with ternary Portland cement-high volume fly ash-calcium carbonate blends. *Case Studies in Construction Materials, 13*, e00426. doi:https://doi.org/10.1016/j.cscm.2020.e00426

S. L. Sarkar, A. K. D. K. D., & Banerjee, G. (1995). Utilization of Fly Ash in the Development of a Cost-Effective Cementitious Product. *ACI Symposium Publication, 153*. doi:10.14359/1082

Saha, A. K. (2018). Effect of class F fly ash on the durability properties of concrete. *Sustainable Environment Research, 28*(1), 25-31. doi:https://doi.org/10.1016/j.serj.2017.09.001

Shang, J., Zhao, K., Zhang, P., Guo, W., & Zhao, T. (2021). Flexural behavior of plain concrete beams containing strain hardening cementitious composite layers with High-Volume fly ash. *Construction and Building Materials, 286*, 122867. doi:https://doi.org/10.1016/j.conbuildmat.2021.122867

Soni, R., Bhardwaj, S., & Shukla, D. P. (2020). Chapter 14 - Various water-treatment technologies for inorganic contaminants: current status and future aspects. In P. Devi, P. Singh, & S. K. Kansal (Eds.), *Inorganic Pollutants in Water* (pp. 273-295): Elsevier.

Sun, J., Jin, N., Tian, Y., & Jin, X. (2012). Experiment Study on Capillary Absorption of Fly Ash Concrete at Different Curing Ages. *Advanced Materials Research, 450-451*, 78-81. doi:10.4028/scientific5/AMR.450-451.78

Thomas, M. (2007). Optimizing the use of fly ash in concrete. *Journal of Materials Science and Chemical Engineering, 5*.

Thomas, M., Jewell, R., & Jones, R. (2017). 5 - Coal fly ash as a pozzolan. In T. Robl, A. Oberlink, & R. Jones (Eds.), *Coal Combustion Products (CCP's)* (pp. 121-154): Woodhead Publishing.

Vimonsatit, S., Chindaprasirt, P., Ruangsiriyakul, S., & Sata, V. (2015). Influence of fly ash fineness on water requirement and shrinkage of blended cement mortars. *KKU Engineering Journal, 42*. doi:10.14456/kkuenj.2015.37

Wang, A., Zhang, C., & Sun, W. (2004). Fly ash effects: III. The microaggregate effect of fly ash. *Cement and Concrete Research, 34*(11), 2061-2066. doi:https://doi.org/10.1016/j.cemconres.2003.03.002

Wei, Y., Chai, J., Qin, Y., Li, Y., Xu, Z., Li, Y., & Ma, Y. (2021). Effect of fly ash on mechanical properties and microstructure of cellulose fiber-reinforced concrete under sulfate dry–wet cycle attack. *Construction and Building Materials, 302*, 124207. doi:https://doi.org/10.1016/j.conbuildmat.2021.124207

Yao, Z. T., Ji, X. S., Sarker, P. K., Tang, J. H., Ge, L. Q., Xia, M. S., & Xi, Y. Q. (2015). A comprehensive review on the applications of coal fly ash. *Earth-Science Reviews, 141*, 105-121. doi:10.1016/j.earscirev.2014.11.016

Yoo, S.-W., Ryu, G.-S., & Choo, J. F. (2015). Evaluation of the effects of high-volume fly ash on the flexural behavior of reinforced concrete beams. *Construction and Building Materials, 93*, 1132-1144. doi:https://doi.org/10.1016/j.conbuildmat.2015.05.021

Yu, Z., Ma, J., Ye, G., Breugel, K., & Shen, X. (2017). Effect of fly ash on the pore structure of cement paste under a curing period of 3 years. *Construction and Building Materials, 144*, 493-501. doi:10.1016/j.conbuildmat.2017.03.182

Zierold, K., & Odoh, C. (2020). A review on fly ash from coal-fired power plants: chemical composition, regulations, and health evidence. *Reviews on environmental health, -1*. doi:10.1515/reveh-2019-0039